We are IntechOpen,
the world's leading publisher of
Open Access books
Built by scientists, for scientists

6,100
Open access books available

149,000
International authors and editors

185M
Downloads

Our authors are among the

154
Countries delivered to

TOP 1%
most cited scientists

12.2%
Contributors from top 500 universities

CLARIVATE ANALYTICS
BOOK CITATION INDEX
INDEXED

WEB OF SCIENCE™

Selection of our books indexed in the Book Citation Index
in Web of Science™ Core Collection (BKCI)

Interested in publishing with us?
Contact book.department@intechopen.com

Chapter

Fluorescent Dextran Applications in Renal Intravital Microscopy

Peter R. Corridon

Abstract

Dextrans, which is a generic term used to describe a family of glucans, are branched polysaccharide molecules derived from lactic acid bacteria in the presence of sucrose. These complex branched glucans have various uses in the medical industry, including plasma expanders and anticoagulants, and have also been investigated for their utility in targeted and sustained delivery of drugs, proteins, enzymes, and imaging agents for renal applications. Simultaneous advances in renal intravital microscopy have brought several advantages over in vitro and ex vivo models by providing real-time assessments of dynamic processes at the cellular and subcellular levels. Such advances have been used to support regenerative medicine strategies. Consequently, this chapter aims to provide an overview of how fluorescent dextrans have supported renal gene and cell therapies and evolving tissue engineering techniques.

1. Introduction

Historically dextrans have been extensively used in clinical practice and experimental models. These compounds can be prepared in a wide range of molecular weights to support their application throughout the vasculature. For instance, intravascular infusions of relatively large molecular weight dextrans have been used as plasma expanders in hypovolemic treatments, substitutes for whole blood in cases of severe shock, and a mode to combat volume depletion in various conditions [1–7]. In contrast, low molecular weight dextrans, which can be filtered by the glomerulus and reclaimed by the tubules, have found use in nephropathology evaluations in experimental and clinical approaches [8–17]. Moreover, within other branches of the medical industry, these complex branched glucans possess properties that support anticoagulation and allow them to be effectively used as vehicles for the targeted and sustained delivery of drugs, proteins, enzymes, and imaging agents [6, 18].

Simultaneously, microscopy advances, particularly intravital microscopic techniques, have brought several advantages over in vitro and ex vivo models by providing instant assessments of dynamic cellular and subcellular events in vivo [13, 14, 19–23]. As we have also improved our capacities to induce genetic alterations within the past

two decades effectively, new opportunities have arisen to, in turn, improve our fundamental understanding of mechanisms that drive disease progression and define novel gene- and cell-based strategies to combat these debilitating outcomes. To date, it can be argued that renal intravital microscopy (IVM) has benefited substantially from the intersection of these approaches. Consequently, this chapter can provide insight into how fluorescent dextrans have supported the development of renal gene and cell therapies and describe how these approaches are impacting the evolving field of regenerative medicine, specifically within the realm of whole organ bioengineering.

2. How optical microscopic techniques have advanced kidney imaging

2.1 Optical microscopy

Optical microscopy systems can be classified into two major categories: linear and non-linear. Traditionally, confocal fluorescence and wide-field laser microscopy systems have been regarded as the most prominent applications [24], and such linear techniques are extensively applied in in vitro studies focused on cell culture and tissue sections. One major challenge with these approaches revolves around spatial resolution. Spatial resolution is generally restricted and merely provides a viable imaging depth from the specimen's surface of roughly 100 μm. Compounded scattering events constrain light propagation and hinder image acquisition at greater depths [25]. Such characteristics limit in vivo applications and the overall clinical utility of these systems. Specifically, these matters are of particular significance to confocal microscopic applications, which rely on the light emanating from the sample that is, in turn, channeled to the pinhole. High degrees of scattering generated in turbid media are well-correlated with tissue depth in biological tissues [13], which also limits the intensity of light that can propagate through the pinhole, thereby severely attenuating the optical signals.

Non-linear microscopic approaches, by comparison, offer the use of higher-order light-matter interactions with multiple photons. This process inherently enhances image-based contrast and, as a result, considerably surmounts the obstacles hindering tissue imaging at greater depths [26]. This principle is widely applied in multiphoton (namely, two-photon) absorption fluorescence excitation techniques that utilize quadratic (non-linear) relationships between excitation and emission events [27, 28]. In doing do, two-photon systems facilitate investigations in tissues at imaging depths on the order of a millimeter, significantly exceeding conventional single-photon processes like confocal microscopy. These systems require the simultaneous absorption of two photons for this excitation process to generate emissions that vary with the square of the excitation intensity.

Multiphoton imaging thus provides several benefits over its counterparts, including reduced scattering levels with infrared-derived excitations, out-of-focus photobleaching, and background fluorescence produced by localized excitations [17]. Overall, these benefits have supported multiphoton imaging over other light-based microscopy systems for live biological tissue examinations, permitting deep tissue imaging at a high resolution. Furthermore, this advanced imaging technique aids the monitoring of live physiological/pathophysiological cellular and subcellular events in real-time. It is precisely for these reasons that multiphoton fluorescence microscopy has gained widespread application in the intravital imaging of the kidney. These applications include analyzing normal renal physiology [13, 28, 29] and pathophysiology [30], and specifically, the quantification of acute, chronic, and end-stage

disorders [16, 31], molecular biodistributions, and effects of various drug development [32], monitoring renal genetic alterations, and most recently tissue engineering [33].

2.2 Intravital microscopy

Advanced imaging technologies, such as multiphoton microscopy, have given researchers powerful tools to answer critical problems in live systems. One such tool is IVM. This form of optical microscopy provides investigations at the cellular and subcellular levels [34]. The development of such non-linear approaches has resulted in a considerable surge of in vivo investigations to tackle fundamental issues in various organ systems [35].

IVM has demonstrated tremendous utility in studying innate and adapted morphology and functional processes among all forms of microscopy. IVM, in particular, has revolutionized our knowledge of living systems through detailed dynamic insights on various regulatory processes [36–40], as well as in-depth anatomical distinctions that support these processes. Non- or minimally-invasive multiphoton systems generate high contrast images with exquisite lateral spatial resolutions that can be adapted to acquire three-dimensional volumes in time-dependent manners [24]. These facts make this system well-suited for tissue, cellular, and molecular studies [41] and have developed new avenues for studying live systems in physiological and pathophysiological conditions, particularly within the kidney, through enhanced live four-dimension applications. Therefore, it is believed that this modality will continue to transform this industry as new ways are being sought after to improve image acquisition time and imaging depth and reduce the complexity and cost of these systems, Overall, these benefits can, someday, drive its clinical potential and utility in the field of biomedicine [41].

3. Fluorescent dextrans and intravital microscopy

3.1 The dextran

One major component that has helped advance this fields of study is the dextran. Dextrans are complex branched glucans produced from glucose polymers via chemical synthesis or from the bacterium Leuconostoc mesenteroides action on sucrose bacteria [18]. These polysaccharides are primarily made up of linear α-1,6-glucosidic linkages with various degrees of branching. Specifically, the glucose subunits are linked by $\alpha(1 \rightarrow 6)$ linkages on its main chain and $\alpha(1 \rightarrow 3)$ linkages on its side chain [42]. Their polymerization is catalyzed by the enzyme dextransucrase and can occur in several microorganisms to produce compounds that vary in molecular weight. The resulting dextrans can also vary in branching patterns, from slightly to highly branched structures.

The polydispersity of dextrans is another physicochemical feature that influences their behavior in vivo and their excellent biocompatibility. Dextran polymers are generally stable under normal, as well as mildly acidic and basic conditions. Dextrans also contain a significant number of hydroxyl groups for conjugation, supporting their high-water solubility. These heterogeneous polysaccharides are biodegradable and can be cleaved by various dextranases. Altogether these properties have supported their preclinical and clinical use for the past several decades.

3.2 Clinical- and research-based applications of dextran molecules

Dextrans produce relatively low-viscosity solutions and are generally classified as neutral polymers. Based on this classification, dextrans are versatile compounds with many clinical applications in anesthesiology, radiology, ophthalmology, and emergency medicine. Typically, these compounds cannot penetrate the intact membranes of living cells. As a result, they can be used to evaluate membrane dynamics, and macromolecular distributions and kinetics [43]. Specifically, large molecular weight dextrans in the plasma can be used to assess and mimic the properties of the circulation in both normal and pathological conditions [44].

Initially, these molecules were used as colloids for fluid resuscitation as they osmotically expand the plasma and help restore blood plasma volume post severe hemorrhage [45]. These compounds distribute throughout the circulation, expand blood volume, and thus, increase cardiac output and blood flow. However, these polymers appear to impede fibrin network formation by increasing this protein's degradation. Research has also shown that the significant presence of dextran molecules leads to decrements in von Willebrand factor altering platelet funcion [46]. As a result, a move that supported their general abandonment in such settings arose from the abovementioned issues, along with the adverse effects these compounds had on the innate coagulation system and their potential to induce anaphylactic responses [46]. Interestingly, this antithrombotic effect provides additional clinical utility for preventing postoperative venous thrombosis.

From a medical imaging perspective, these compounds can be labeled with various markers to support various non-invasive detection and diagnostic techniques. For instance, the intravenous delivery of dextrans labeled with technetium Tc-99 m serves as contrast agents for nuclear medicine, magnetic resonance imaging, or scintigraphy investigations [46]. Whereas, from a microscopic perspective, fluorescently-labeled dextrans have been widely used to support countless investigations within the kidney, which is the focus of this chapter. That is, dextrans are easily modified to accept fluorophores that can be used to label various renal compartments exclusively based on molecular weight. Specifically, this property facilitates the study of microvascular flow, vascular integrity, vesicular trafficking, glomerular filtration, and renal reabsorption and secretion [35]. Examples of some commonly used fluorescent dextrans are provided in **Figure 1**.
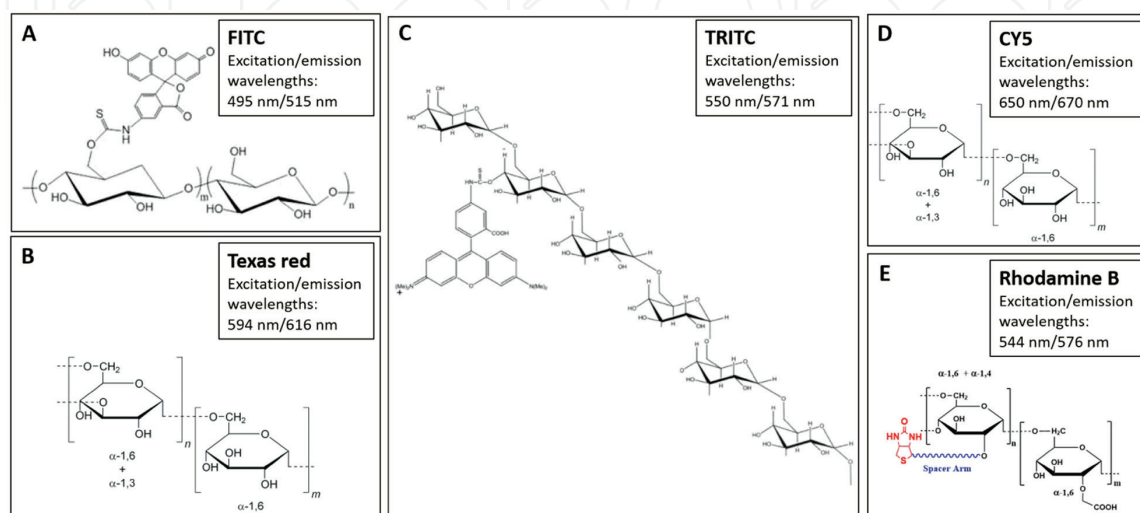

Figure 1.
The structures of some commonly used fluorescent dextrans. This image depicts the following fluorescently conjugated dextrans: (A) FITC, (B) Texas red, (C) TRITC, (D) cyanine 5 (CY5), and (E) rhodamine B.

3.3 Intravital multiphoton fluorescence microscopy fundamentals

The fields revolving around biological fluorescence have a rich and vibrate history that dates back to original observations presented in 1565 by Nicolas Bautista Monardes, botanist and physician [47]. Monardes' article communicated the simple outlines of various visible hues emanating from several wood types. However, such observations provided a means to detect counterfeit samples from scarce and valuable materials, like coatli, known for its diuretic properties. This simplified approach relied on a crucial characteristic of the counterfeit materials: their ability to emit clear blue hues after being immersed in water [48]. This characteristic was beneficial and undoubtedly paved a path for contemporary optical advancements.

As various fields in optics advanced, two noteworthy processes, incandescence and photoluminescence, have been defined. Incandescence describes a thermal radiative process that supports the generation of electromagnetic radiation from the thermal motion of charged particles within substances. The resulting electromagnetic radiation emanates from the visible spectrum and occurs as a consequence of elevations in temperature. Such a heat response generates increased particle motion, giving these particles a more remarkable ability to radiate. In comparison, photoluminescence also describes optical emissions via electronic state transitions, albeit in a manner that is independent of heat and is deemed a cold process. Due to this nature, this phenomenon was the center of much debate two centuries ago, when scientists vehemently argued about the applicability of photoluminescence within the realm of thermodynamics [48]. Nevertheless, we have witnessed the use and classification of several aspects of photoluminescence, namely, resonant radiation, phosphorescence, and fluorescence, which permeate our daily lives. Each of these three processes will be briefly outlined below.

We can first focus on the theory related to the swift emission of electromagnetic energy derived from the photonic absorption of gaseous atoms, upon which resonant radiation centers. Within this process, incident photons, generally, possess the same or perhaps frequencies similar to the resonant frequencies of the gaseous atoms, allowing them to first transition to higher energy levels after radiation absorption, and subsequently relax to a lower energy state. The latter transition is accompanied by the emission of photons with energy levels comparable to incident particles, eliminating substantial energy decrements during these transitions and defining discrete energy differentials. These discrete demarcations are characteristic of a given atom and thus provide unique energy transition signatures. Next, with phosphorescence, photonic emission results in a reduction of energy states. Compared to resonant radiation, in this excitation process, the emitted photons possess lower energy levels than their counterparts and generally occur on a longer timescale, allowing phosphorescent materials to discharge radiation for extended periods post excitation.

Building on the previously mentioned description provided on resonant radiation, we can first begin to examine one-photon or conventional fluorescence further. In this process, a single photon is absorbed by a fluorophore. Fluorophore atoms comprise electrons occupying various specific electronic states, defining their perpetual vibrational, rotational, or translational motions that occur in relation to the physical state of the fluorescing compound(s). Notably, the excitation of a fluorophore (or a luminophore) can occur through either single or multiphoton absorption events, and once a fluorophore absorbs a photon, a resulting electronic energy transition will occur. The probability that such a fluorophore will collide with surrounding molecules to support its relaxation is increased upon transitioning to a higher energy level.

Likewise, the de-excitation process can, in turn, be defined in three phases. Within the first phase, some of the absorbed energy can facilitate fluorophores' vibrational/ rotational modes as well as heat generation from internal conversion-based radiative decay or radiationless de-excitation. The second phase commences and revolves around energy losses/conversion processes required to produce photons, as defined by the Stokes shift, which exists with energy levels lower than those of their incident counterparts. Ultimately, in this form of de-excitation, the third phase is characterized by an additional internal conversion process that further reduces the particles' energy states.

As a result, we can thus compare the processes mentioned above to the multiphoton phenomena utilized in IVM. With IVM, fluorescence is derived from the absorption of two or more low-energy photons concurrently. This combination is essential as each photon's energy is incapable of generating an excitation event, yet when combined, the resulting energy level is sufficient to facilitate this electronic transition. Moreover, as observed in single photon fluorescence, the de-excitations result in photonic emissions described in detail in the literature [28, 38, 39, 49].

3.4 Practical ways to generate multiphoton excitation fluorescence

In order to generate a multiphoton excitation event, the required photons must be absorbed by the fluorophore within a single attosecond. This constraint drastically minimizes the probability of naturally occurring multiphoton phenomena. To illustrate this point, if we expose a rhodamine molecule to direct sunlight, we can expect a one-photon excitatory event to occur within a timeframe of 1–2 seconds, whereas a two-photon event would occur after 10 million years [6, 11]. These depictions were revealed in 1931 by Dr. Marie Groppert-Mayer. She simultaneously forecasted that an enormous flux of incident radiation could overcome this 10 million-year period to produce detectable levels of multiphoton fluorescence in a time frame comparable to the one-photon excitatory event [28, 38, 39, 49].

Dr. Groppert-Mayer's models devised the underpinning framework upon which femtosecond laser technologies have been developed. Today, these robust systems, like titanium: sapphire lasers, produce high and sustained photon fluxes of energy required that facilitate routine multiphoton excitations/emissions from femtosecond pulses. The concise duration in which these infrared systems emit light pulses inherently only generates photon fluxes that can raise the temperature of water by, on average, 0.2 K/sec [28]. Furthermore, exposure to phototoxic effects is limited by the fact that long wavelength, low-energy photons are constricted to minimize scattering and improve depth penetration and resolution for safe and effective biological studies. Compared to the two-photon excitation, in single-photon excitation, tissues are generally exposed to far more levels of shorter wavelength and higher energy, ultraviolet and visible light with lasers that excite fluorophores within substantially greater volumes that subject tissues to more debilitating events. Excitingly, these benefits have propelled research to develop three-photon systems that require roughly 10-fold photon densities applied in two-photon microscopic applications and promise enhanced depth penetration and resolution [50].

3.5 Image formation in multiphoton fluorescence microscopy

The next step in the IVM process revolves around image acquisition. This process converts the optical signals that emanate from a sample to electrical signals. Extensive

details of this process can be obtained in the literature [51], and for the purposes of this chapter, the fundamental concept is outlined as follows. First, it is essential to identify key components of a multiphoton fluorescence microscopy system that support image acquisition and formation. These components are the objectives, the mirrors, and the detectors, which are utilized in a subsequent manner.

After the mode-locked/pulse femtosecond laser emits incident radiation, scanning dichroic mirrors are used to guide the beams of light onto various objective lenses. These lenses then focus the beams at unitary loci within the sample. As theorized by Dr. Groppert-Mayer, this process directs enormous fluxes of incident radiation on the specimen in both spatially and temporally fashions and facilitates multiphoton fluorescence excitation events that emit photon beams. Despite applying enormous quantities of incident radiation, the system's average input power is delimited below 10 mW via low pulse duty cycles and coincides with the power levels generated by confocal systems. Also, since most photons follow a direct path, multiphoton systems have drastically enhanced signal-to-noise ratios compared to one-phase microscopy systems.

Further comparisons to confocal fluorescence microscopy identify the absence of a pinhole in IVM systems. The alternative configuration provides more flexibility in designating the detection geometry to incorporate descanned or non-descanned detection schemes. Non-descanned systems provide a means to enhance depth penetration and reduce the number of optical elements needed and the path length that emerging fluorescence signals can interact with dust particles, thereby limiting losses to scattering and improving the sensitivity of the system light and efficiency of light collection. This process enhances sensitivity without compromising image quality. It is essential for maximal depth penetration into living tissue, as the detectors contain susceptible photomultiplier tubes capable of detecting low levels of light and barrier filters that are used to generate red, green, and blue pseudo-color images formed from a 3-D geometrical correlation within a given specimen. Two-dimensional, XY-plane raster scanning processes support data acquisition that can be coupled with depth position (Z-plane). The resulting imaging datasets can be extended to 4-D investigations by acquiring data in a time-dependent manner.

3.6 In vivo multiphoton imaging of mammalian tissues and its benefits over ex vivo and in vitro approaches

Historically, researchers have relied on in vitro, ex vivo, and in vivo experimental models to answer scientific questions that have and continue to improve our mechanistic understanding of various physiological processes. Such work has spearheaded advancements that, for example, have allowed the examination of complex cellular-molecular interactions in vitro. In vitro characterizations provide opportunities to conduct high-throughput, cost-effective studies that are the first and integral initial step that circumvents complex intracellular, intercellular, intra-organ, and inter-organ events within live animal models. After that, such approaches can be transitioned to comparable ex vivo and, ultimately, in vivo models. Experimental approaches of this nature provide greater degrees of flexibility and facilitate ways to view complex phenomena more straightforwardly and systematically, and conduct practices that would be impractical for animal studies that may not be approved for animal usage by regulatory boards.

Nevertheless, in vitro and ex vivo models, by their very nature, are incapable of fully mimicking natural phenomena. The fact illustrates the trade-off that must be

considered when solely relying on this form of experimentation and the need to apply multiple approaches when studying complex biological systems [52]. As a result, IVM has gained more prominence. These live imaging systems have equipped researchers with a means to acquire unique and compelling evidence that can only be gathered from whole organ investigations [9]. IVM's current utility can be extended through more invasive approaches that support organ exposure/exteriorization that can be conducted on rodent brains [53–55], livers [56–58], and kidneys [9, 58–60], as well as ex vivo applications that extend depth penetration of existing IVM systems. Besides these accomplishments, IVM is currently a niche platform that can only be performed non-invasively on shallow tissue depths and easily accessible organs like the skin [61–63].

The preparations to conduct such imaging studies are crucial in ensuring the generation of valuable microscopic data. In particular, intravital multiphoton imaging of kidney function and structure has become quite popular since the kidneys of rats and mice can be easily externalized after anesthesia and placed in the view of a microscope lens [12, 28, 35, 64, 65]. To conduct such studies, it is important to outline some of the following essential conditions that include the use of anesthesia, analgesics, and antiseptics, as well as other common surgical considerations that should be considered. Generally, standalone or combinative inhalable (isoflurane, for short duration studies) and injectable (for more extended duration studies: pentobarbital – for survival studies or thiobutabarbital – for terminal studies) sedatives are used for small animal studies. Analgesics like acetaminophen and antiseptics, like a surgical scrub, are also routinely used at the end of survival studies. Researchers should also compensate for fluid losses by introducing isotonic fluids and serum albumin to regulate osmotic pressures.

It is generally recommended to conduct surgical procedures in sterile environments, especially for survival studies. After fully sedating the rodent, one should constantly monitor its core temperature, often done with an anal probe, along with heating pads, lamps, and blankets to regulate core temperature during the surgical and imaging procedures. A carotid or femoral artery access catheter can also monitor blood pressure. Further safeguards may be taken by sterilizing the imaging dish and saline in which externalized kidneys are placed to limit infection and tissue dehydration/pH alterations.

4. Materials and methods for intravital studies

4.1 Animals and associated procedures for intravital studies

Primarily male Sprague Dawley rats (Harlan Laboratories, Indianapolis, IN), as well as Frömter Munich Wistar (Harlan Laboratories, Indianapolis, IN) and Simonsen Munich Wistar (Simonsen's Laboratory, Gilroy, CA) rats are used for these types of studies. These animals generally range in weight from 150 to 450 g. Wistar rats are used for glomerular studies due to the unique abundance of superficial glomeruli that can be easily accessed using this imaging technique. Additionally, all animals should be given free access to standard rat chow and water (unless the model requires otherwise, and most importantly, all experiments must be conducted under the approval of institutional animal care committees and welfare guidelines. These approaches can be adjusted for studies in other rodents, namely, mice. However, for this chapter, we will focus on rat models.

4.2 Fluorescent dextran marker preparation and infusions

Various conjugated dextrans, which vary according to the fluorescent tag and molecular weights, can be used for intravital two-photon fluorescent imaging studies. For example, single or combinations of the following dextrans can be applied to examine vascular integrity and routine renal filtration capacities: 3 kDa Cascade Blue, and 4 and 5 kDa Fluorescein Isothiocyanate (FITC) dextrans (Invitrogen, CA); and 150 kDa Tetramethyl Rhodamine Isothiocyanate (TRITC) dextran (TdB Consultancy, Uppsala, Sweden). It is recommended first to produce a stock solution that can be used in an imaging study with a concentration of 20 mg/ml, from which 500 μl can be diluted in 1 ml of isotonic saline [66]. Care should also be taken to ensure that the molecular weight of large dextran molecules should not be dispersed over a wide range, as such variations can support renal ultrafiltration and incorrectly report filtration and reabsorption capacities.

In live rats, two main modes of infusions are supported via jugular and tail veins (**Figure 2**). For jugular vein infusions, it is vital first to anesthetize the rat using isoflurane in 5% oxygen (Webster Veterinary Supply, Inc., Devens, MA). After this initial sedation, the animal's core temperature (approximately 37°C) should be regulated with a heating pad (**Figure 2**), and an intraperitoneal injection can be given for survival (50 mg/kg of pentobarbital) or non-survival (130 mg/kg thiobutabarbital) procedures. Once the rat is completely stabilized, the researcher can shave its neck and sanitize the region using a common antiseptic like Betadine Surgical Scrub (Purdue Products L.P., Stamford, CT). Incisions can then be made to expose and isolate the jugular vein with 3–0/4–0 silk loops. Common practice is applying a superior loop that can be tied and clamped with a pair of hemostats to stiffen and elevate this vein. After that, a minor incision can be made to facilitate the insertion of a PE-50 tubing catheter, which is attached to a 1 ml syringe containing injectate, into the jugular vein. Another silk loop can be applied to anchor the catheter further. Similarly, tail vein infusions can be conducted post sedation by moistening the tail with a warmed sheet of gauze or placing it into a warm bath to support dilation. Once dilated, A 25-gauge butterfly needle attached to a syringe containing injectates can be inserted into this vein to support the delivery of infusates.

Analogously, hydrodynamic retrograde renal vein fine-needle injections have been defined to facilitate renal cell, and gene transplantation [16, 17, 67]. In this process, intraperitoneal incisions are performed to isolate and occlude venous segments using delicate and non-traumatic micro-serrefine clamps of the left renal hilus. First renal artery is clamped, and then the renal vein. The vein is then elevated with either 3–0 or 4–0 silk loops to support rapid injections into this outport. The needle can then be removed, and pressure applied to the injection site using a cotton swab to induce hemostasis. Further details of this technique are outlined in the literature [16, 17, 67]. Lastly, the vascular clamps can be removed (the venous clamp should be removed before the arterial clamp) to restore flow. The total clamping should be less than 3 minutes and the midline incision can be closed to allow the animal to recover.

4.3 Renal intravital two-photon fluorescence microscopy

In anesthetized rats, the left flank should be shaved, and vertical incisions need to be created to externalize the left kidney. A heating pad can then be placed over the rat to maintain its core temperature. The investigator can then place the kidney inside a glass bottom dish with saline, that is set above either a 20X or 60X water immersion
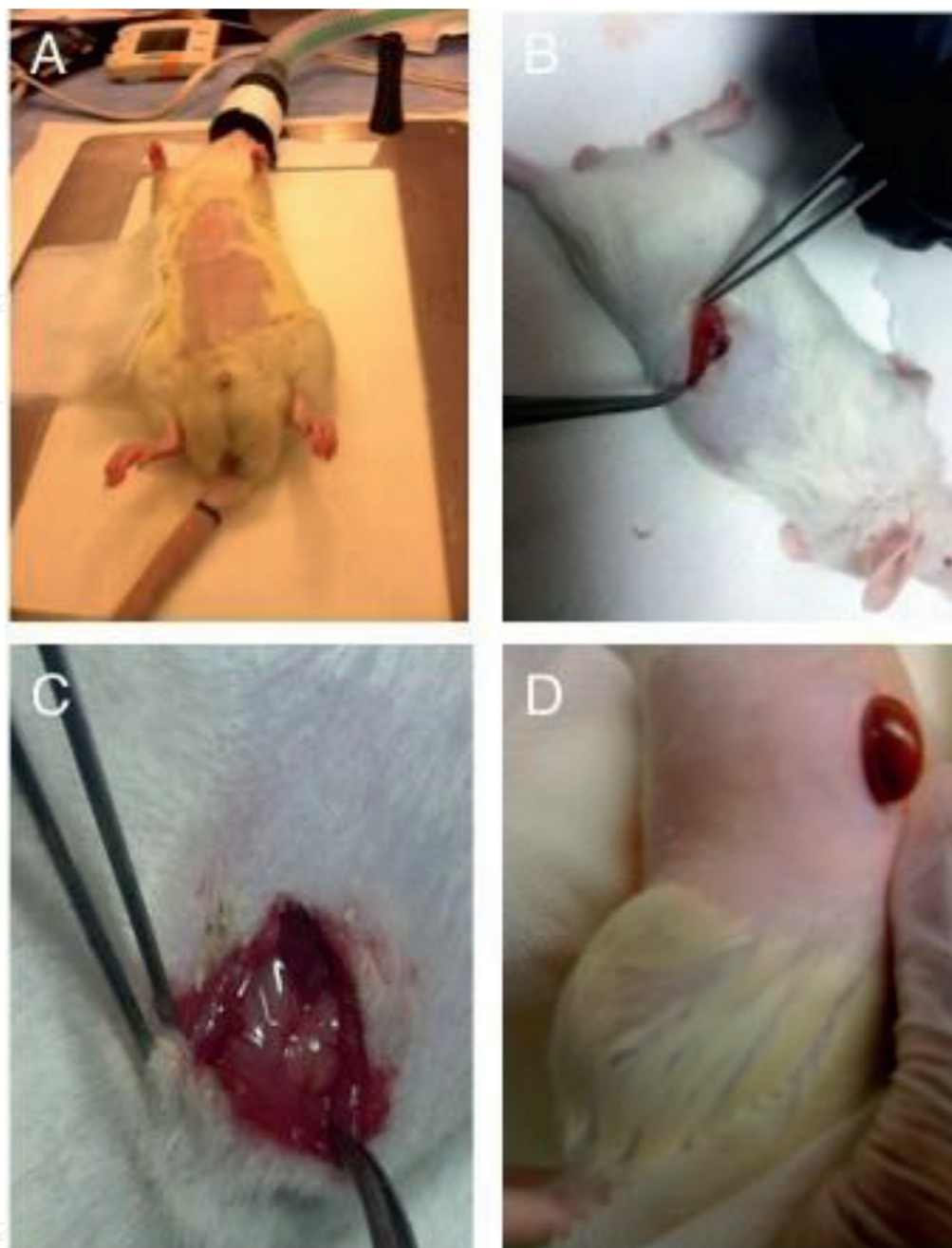
Figure 2.
Digital images illustrate common surgical procedures applied to exteriorize the rat kidney for intravital imaging. These images transition from the provision of inhaled anesthesia that sedates the animal and prepares it for surgery (A); to the generation of a flank incision that facilitates the exteriorization of the left kidney (B through D). Digital zoom provides greater detail in image (C) of the field presented in image (B) by accentuating the tuft of perirenal fat situated at the apex of the kidney that is used to gently birth the kidney from the flank incision, as presented in image (D).

objective for imaging, with the animal's body acting as a weight to stabilize kidney position [16, 65, 66] (**Figure 3**).

Fluorescent images can be acquired from externalized organs. Then, measurements can follow an Olympus FV 1000- MPE Microscope set with a Spectra-Physics Mai Tai Deep See laser, tunable from 710 to 990 nm, with dispersion compensation for two-photon microscopy (Olympus Corporation, Tokyo, Japan). The system in question is generally accompanied by a pair of external detectors for multiphoton imaging and dichroic mirrors for collecting blue, green, and red emissions. The emitted light is
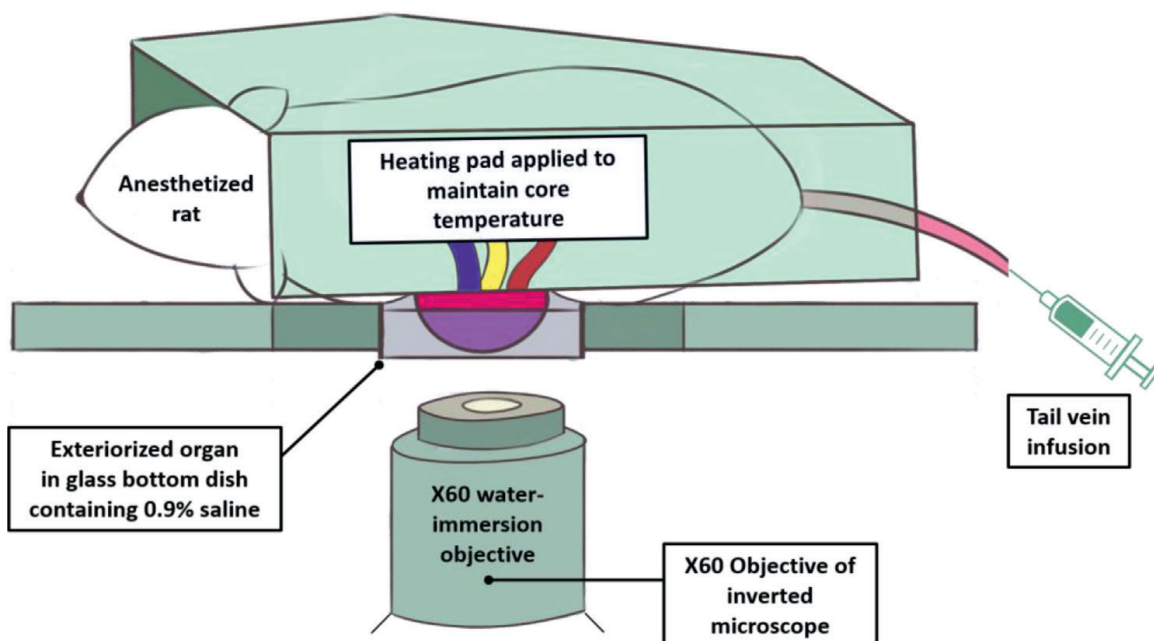
Figure 3.
A schematic illustrating the renal IVM process. In this image, an anesthetized rat, covered with a heating pad to maintain core temperature, has its left kidney exteriorized and placed in a 50 mm glass-bottom dish, filled with saline, and set above the stage of an inverted microscope with a Nikon ×60 1.2-NA water-immersion objective. A 25-gauge butterfly needle was inserted into the dilated tail vein and attached to a syringe containing injectates.

collected using a 3-fixed bandpass filter system: 420–460 nm (blue channel), 495–540 nm (green channel), and 575–630 nm (red channel). The system can be mounted on an Olympus IX81 inverted microscope for conducting live imaging.

5. Renal gene and cell therapies and evolving tissue and engineering techniques devised using fluorescently-tagged dextrans

Concurrently, advances in renal IVM have brought several advantages over in vitro and ex vivo models by providing real-time assessments of dynamic processes at the cellular and subcellular levels. These advances have relied on dextrans to optimize exogenous gene/cell delivery methods, tissue functionality following these alterations, and whole bioengineered organ scaffold integrity. Such advances have been applied to support regenerative medicine strategies, namely renal gene and cell therapies, as well as tissue engineering.

5.1 Optimization of exogenous gene/cell delivery methods

Previous studies that were used to verify that hydrodynamic delivery facilitates robust exogenous transgene and cell distribution throughout the live rodent kidney were based on the internalization of low-, intermediate-, and high-molecular-weight exogenous macromolecules. These infusates were comparable to transgene and transcell suspension [17]. Such studies presented overwhelming evidence that hydrodynamic injections augmented with vascular cross clamps can consistently induce cellular uptake of exogenous low, intermediate, and large macromolecules in numerous live nephron segments.

Interestingly, this rapid injection method supported the robust apical cellular internalization of large-molecular-weight dextran molecules like the incorporation of low-molecular-weight dextran, along with intense basolateral distributions. Data also provided evidence that large molecular-weight dextran molecules could atypically access the tubule lumen at high concentrations after being delivered to the kidney. Likewise, the introduction of large molecular weight, 150-kDa, dextran molecules into the vasculature before hydrodynamic delivery facilitated their internalization within tubular epithelial cells after the injection process was conducted using iso-tonic saline. Nevertheless, such atypical access to tubular epithelium and lumen was transient and appeared to only occur as a consequence of the hydroporation process. Such results highlight possible delivery routes of transgene entry that can support renal genetic transformation induced by hydrodynamic injections.

These versatile and fluorescently-tagged molecules also helped examine correlations between hydrodynamic injection parameters and reliable transgene expression/ cellular incorporation. Specifically, the conditions required to infuse the transgenes at various injection rates were examined to provide insight into each infusion rate's effectiveness and impact on renal structure and function. The resulting data were compared to standard systemic fluid delivery to the kidney in normal rats via jugular and tail vein infusions. The high molecular weight (150-kDa) fluorescent dextran molecules were delivered systemically via either venous route and were characteristically restricted within the peritubular capillaries surrounding intact proximal and distal tubules. This probe was widely distributed within the vasculature of nephron segments that were accessible for imaging by our two-photon microscope independent of the infusion method. This imaging technique can extensively survey the distribution of the fluorescent dye as a function of renal tissue depth.

5.2 Examination of tissue functionality following exogenous gene/cell delivery

In comparison, after identifying a time course for renal recovery and viable delivery, it was necessary to investigate whether these processes would hinder intrinsic renal structural and functional capacities. For this, systemically introduced fluorescent low/large molecular weight dextrans helped investigate the potential uptake and distribution of dyes in superficial nephron cross sections in animals that received hydrodynamic retrograde injections.

Studies were presented to confirm whether this gene delivery method can induce significant degrees of injury. For such studies, morphological and functional assays were conducted 3–28 days post-non-viral and viral hydrodynamic injections to examine microvascular integrity and metabolically activity after gene delivery and expression. Rats received jugular/tail vein infusions of 150-kDa and 3-kDa dextrans to detect augmentations to native renal filtration and endocytic uptake capacities. These studies revealed the maintained innate capacities in each case, as the 3-kDa dye was rapidly filtered and endocytosed by the proximal tubule epithelia, and the 150-kDa dye was retained within the peritubular vasculature. Such results are consistent with normal renal function [12, 16, 17]. Nephron structure and function appeared normal after hydrodynamic delivery, transgene expression, and cellular incorporation.

A significant result from these experiments revealed that the low-molecular-weight dextran molecules were taken up equally well by cells that either did or did not express fluorescent proteins in rats treated with various types of transgene vectors (plasmid and adenovirus vectors). This characteristic indicated that these cells retained functional activity. Again, the data are consistent with endocytic uptake of

low molecular weight dextran molecules in rat kidneys [9, 12, 13, 16, 17, 65]. These observations showed that nephron segments could retain vital functional capacities after rapid fine-needle, hydrodynamic venous delivery. Alternatively, this cell delivery technique can also be used to establish tumor models in this organ, thereby providing an extension of its utility [68].

5.3 Evaluation of whole bioengineered organ scaffold integrity

Efforts in tissue engineering have heightened the desire for alternatives such as the bioartificial kidney [69–72]. Whole organ decellularization has been described as one of the most promising ways of constructing a bioartificial kidney [73]. Decellularization focuses on extracting the extracellular matrix (ECM) from the native kidney with as many structural and functional clues as possible. The ECM can then be employed as a natural template for regeneration, as observed traditionally in commercial substitutes [74].

This technique has gained much attention lately, yet maintaining adequate scaffold integrity in the post-transplantation environment remains a considerable challenge. Specifically, there is still a limited understanding of scaffold responses post-transplantation and ways we can improve scaffold durability to withstand the in vivo environment. Recent studies have outlined vascular events that limit organ scaffold viability for long-term transplantation. However, these insights have relied on in vitro/in vivo approaches that lack adequate spatial and temporal resolutions to investigate such issues at the microvascular level.

As a result, intravital microscopy has been recently used to gain instant feedback on their structure, function, and deformation dynamics [75]. This process was able to capture the effects of in vivo blood flow on the decellularized glomerulus, peritubular capillaries, and tubules after autologous orthotopic transplantation into rats. Large molecular weight dextran molecules labeled the vasculature. They revealed substantial degrees of translocation from glomerular and peritubular capillary tracks to the decellularized tubular epithelium and lumen as early as 12 hours after transplantation, providing real-time evidence of the increases in microvascular permeability. Macromolecular extravasation persisted for a week, during which the decellularized microarchitecture was significantly compromised and thrombosed. These results indicate that in vivo multiphoton microscopy is a powerful approach for studying scaffold viability and identifying ways to promote scaffold longevity and vasculogenesis in bioartificial organs.

6. Conclusions

Dextrans are widely used molecules for various applications within medicine. Traditionally, these complex branched glucans have been used as plasma expanding and antithrombotic agents. In more recent times, their applications have extended to the realm of regenerative medicine, where researchers have found niche roles in developing and evaluating the delivery of novel cell- and gene- therapeutics and imaging agents for in vivo investigations. Developments in optical microscopy have also aligned with these applications to produce exciting opportunities for renal intravital models that have now extended to the field of whole organ bioengineering. As a result, the chapter was used to provide insights into how optical microscopic techniques have advanced kidney imaging, the use of fluorescent dextrans, and intravital microscopy. This approach was supported by illustrating how a well-established

delivery technique supports exogenous gene/cell delivery to the kidney, along with an example of whole organ bioengineering techniques that can be evaluated using IVM. The illustration can be accessed in further detail in the literature. Overall, it is hoped that this chapter will support future regenerative and bioengineering efforts by emphasizing the relevant methodologies needed to conduct these intravital studies.

Acknowledgements

Conflict of interest

The author declares no conflict of interest.

Author details

Peter R. Corridon[1,2,3]

1 Biomedical Engineering and Healthcare Engineering Innovation Center, Khalifa University, Abu Dhabi, UAE

2 Department of Immunology and Physiology, College of Medicine and Health Sciences, Khalifa University, Abu Dhabi, UAE

3 Center for Biotechnology, Khalifa University, Abu Dhabi, UAE

*Address all correspondence to: peter.corridon@ku.ac.ae

IntechOpen

References

[1] Neu B, Wenby R, Meiselman HJ. Effects of dextran molecular weight on red blood cell aggregation. Biophysical Journal. 2008;**95**(6):3059-3065

[2] Isbister JP, Fisher MM. Adverse effects of plasma volume expanders. Anaesthesia and Intensive Care. 1980;**8**(2):145-151

[3] Mays T, Mays T. Intravenous iron-dextran therapy in the treatment of anemia occurring in surgical, gynecologic and obstetric patients. Surgery, Gynecology & Obstetrics. 1976;**143**(3):381-384

[4] Huskisson L. Intravenous volume replacement: Which fluid and why? Archives of Disease in Childhood. 1992;**67**(5):649-653

[5] Tinawi M. New trends in the utilization of intravenous fluids. Cureus. 2021;**13**(4):e14619

[6] Ukkund SJ et al. 1 - dextran nanoparticles: Preparation and applications. In: Venkatesan J et al., editors. Polysaccharide Nanoparticles. Amsterdam, Netherlands: Elsevier; 2022. pp. 1-31

[7] Terg R et al. Pharmacokinetics of Dextran-70 in patients with cirrhosis and ascites undergoing therapeutic paracentesis. Journal of Hepatology. 1996;**25**(3):329-333

[8] Sandoval RM, Molitoris BA. Quantifying glomerular permeability of fluorescent macromolecules using 2-photon microscopy in Munich Wistar rats. Journal of Visualized Experiments. 2013;**74**:e50052:1-7

[9] Dunn KW, Sandoval RM, Molitoris BA. Intravital imaging of the kidney using multiparameter multiphoton microscopy. Nephron. Experimental Nephrology. 2003;**94**(1):e7-e11

[10] Hato T, Winfree S, Dagher PC. Intravital imaging of the kidney. Methods. 2017;**128**:33-39

[11] Hato T, Winfree S, Dagher PC. Kidney Imaging: Intravital Microscopy. Methods in Molecular Biology. 2018;**1763**:129-136

[12] Ashworth SL et al. Two-photon microscopy: Visualization of kidney dynamics. Kidney International. 2007;**72**(4):416-421

[13] Dunn KW et al. Functional studies of the kidney of living animals using multicolor two-photon microscopy. American Journal of Physiology. Cell Physiology. 2002;**283**(3):C905-C916

[14] Sandoval RM, Molitoris BA. Intravital multiphoton microscopy as a tool for studying renal physiology and pathophysiology. Methods. 2017;**128**:20-32

[15] Tanner GA. Glomerular sieving coefficient of serum albumin in the rat: A two-photon microscopy study. American Journal of Physiology. Renal Physiology. 2009;**296**(6):F1258-F1265

[16] Corridon PR et al. Intravital imaging of real-time endogenous actin dysregulation in proximal and distal tubules at the onset of severe ischemia-reperfusion injury. Scientific Reports. 2021;**11**(1):8280

[17] Corridon PR et al. A method to facilitate and monitor expression of exogenous genes in the rat kidney using plasmid and viral vectors. American Journal of Physiology. Renal Physiology. 2013;**304**(9):F1217-F1229

[18] Mehvar R. Dextrans for targeted and sustained delivery of therapeutic and imaging agents. Journal of Controlled Release. 2000;**69**(1):1-25

[19] Vaghela R et al. Actually seeing what is going on – Intravital microscopy in tissue engineering. Frontiers in Bioengineering and Biotechnology. 2021;**9**. DOI: 10.3389/fbioe.2021.627462

[20] Jun YW et al. Addressing the autofluorescence issue in deep tissue imaging by two-photon microscopy: The significance of far-red emitting dyes. Chemical Science. 2017;**8**(11):7696-7704

[21] Small DM et al. Multiphoton fluorescence microscopy of the live kidney in health and disease. Journal of Biomedical Optics. 2014;**19**(2):020901

[22] Hall AM et al. In vivo multiphoton imaging of mitochondrial structure and function during acute kidney injury. Kidney International. 2013;**83**(1):72-83

[23] Schuh CD et al. Long wavelength multiphoton excitation is advantageous for intravital kidney imaging. Kidney International. 2016;**89**(3):712-719

[24] Masters BR. Correlation of histology and linear and nonlinear microscopy of the living human cornea. Journal of Biophotonics. 2009;**2**(3):127-139

[25] Schmitt JM, Knuttel A, Yadlowsky M. Confocal microscopy in turbid media. Journal of the Optical Society of America. A, Optics, Image Science, and Vision. 1994;**11**(8):2226-2235

[26] Helmchen F, Denk W. Deep tissue two-photon microscopy. Nature Methods. 2005;**2**(12):932-940

[27] Denk W, Svoboda K. Photon upmanship: Why multiphoton imaging is more than a gimmick. Neuron. 1997;**18**(3):351-357

[28] Dunn KW, Young PA. Principles of multiphoton microscopy. Nephron. Experimental Nephrology. 2006;**103**(2):e33-e40

[29] Comper WD, Haraldsson B, Deen WM. Resolved: Normal glomeruli filter nephrotic levels of albumin. Journal of the American Society of Nephrology. 2008;**19**(3):427-432

[30] Kang JJ et al. Quantitative imaging of basic functions in renal (patho)physiology. American Journal of Physiology. Renal Physiology. 2006;**291**(2):F495-F502

[31] Wang E et al. Rapid diagnosis and quantification of acute kidney injury using fluorescent ratio-metric determination of glomerular filtration rate in the rat. American Journal of Physiology. Renal Physiology. 2010;**299**(5):F1048-F1055

[32] Medarova Z et al. In vivo imaging of siRNA delivery and silencing in tumors. Nature Medicine. 2007;**13**(3):372-377

[33] Vaghela R et al. Actually seeing what is going on - Intravital microscopy in tissue engineering. Frontiers in Bioengineering and Biotechnology. 2021;**9**:627462

[34] Weigert R et al. Intravital microscopy: A novel tool to study cell biology in living animals. Histochemistry and Cell Biology. 2010;**133**(5):481-491

[35] Molitoris BA, Sandoval RM. Intravital multiphoton microscopy of dynamic renal processes. American Journal of Physiology. Renal Physiology. 2005;**288**(6):F1084-F1089

[36] Giampetraglia M, Weigelin B. Recent advances in intravital microscopy for preclinical research. Current Opinion in Chemical Biology. 2021;**63**:200-208

[37] Mihlan M et al. Surprises from Intravital imaging of the innate immune response. Annual Review of Cell and Developmental Biology. 2022;**38**. DOI: 10.1146/annurev-cellbio-120420-112849

[38] Taqueti VR, Jaffer FA. High-resolution molecular imaging via intravital microscopy: Illuminating vascular biology in vivo. Integrative Biology. 2013;**5**(2):278-290

[39] Shaya J et al. Design, photophysical properties, and applications of fluorene-based fluorophores in two-photon fluorescence bioimaging: A review. Journal of Photochemistry and Photobiology C: Photochemistry Reviews. 2022;**52**:100529

[40] Cai N et al. Recent advances in fluorescence recovery after Photobleaching for decoupling transport and kinetics of biomacromolecules in cellular physiology. Polymers (Basel). 2022;**14**(9). DOI: 10.3390/polym14091913

[41] Dhawan AP, D'Alessandro B, Fu X. Optical imaging modalities for biomedical applications. IEEE Reviews in Biomedical Engineering. 2010;**3**:69-92

[42] Pachekrepapol U, Horne DS, Lucey JA. Effect of dextran and dextran sulfate on the structural and rheological properties of model acid milk gels. Journal of Dairy Science. 2015;**98**(5):2843-2852

[43] Lencer WI et al. FITC-dextran as a probe for endosome function and localization in kidney. The American Journal of Physiology. 1990;**258**(2 Pt 1): C309-C317

[44] Ruben M, Sandoval & Bruce A, Molitoris BA. Fluorescent Dextrans in Intravital multi-photon microscopy. In: Advances in Intravital Microscopy: From Basic to Clinical Research. Weigert R. Editor. Dordrecht: Springer Netherlands; 2014. pp. 205-219.

[45] Lamke LO, Liljedahl SO. Plasma volume changes after infusion of various plasma expanders. Resuscitation. 1976;**5**(2):93-102

[46] Miao KH, Guthmiller KB. Dextran. Treasure Island (FL): StatPearls; 2022

[47] Ghiran IC. Introduction to fluorescence microscopy. Methods in Molecular Biology. 2011;**689**:93-136

[48] Valeur B, Berberan-Santos MN. A brief history of fluorescence and phosphorescence before the emergence of quantum theory. Journal of Chemical Education. 2011;**88**(6):731-738

[49] Marsh PN, Burns D, Girkin JM. Practical implementation of adaptive optics in multiphoton microscopy. Optics Express. 2003;**11**(10):1123-1130

[50] Lakowicz JR et al. Time-resolved fluorescence spectroscopy and imaging of DNA labeled with DAPI and Hoechst 33342 using three-photon excitation. Biophysical Journal. 1997;**72**(2 Pt 1): 567-578

[51] de Grauw CJ et al. Imaging properties in two-photon excitation microscopy and effects of refractive-index mismatch in thick specimens. Applied Optics. 1999;**38**(28):5995-6003

[52] Rothman SS. Lessons from the Living Cell : The Culture of Science and the Limits of Reductionism. New York: McGraw-Hill; 2002

[53] Stutzmann G. Seeing the brain in action: How multiphoton imaging has advanced our understanding of neuronal function. Microscopy and Microanalysis. 2008;**14**(6):482-491

[54] Chia TH et al. Multiphoton fluorescence lifetime imaging of intrinsic fluorescence in human and rat brain tissue reveals spatially distinct NADH binding. Optics Express. 2008;**16**(6):4237-4249

[55] Bacskai BJ et al. Four-dimensional multiphoton imaging of brain entry, amyloid binding, and clearance of an amyloid-beta ligand in transgenic mice. Proceedings of the National Academy of Sciences of the United States of America. 2003;**100**(21):12462-12467

[56] Lin J et al. Assessment of liver steatosis and fibrosis in rats using integrated coherent anti-stokes Raman scattering and multiphoton imaging technique. Journal of Biomedical Optics. 2011;**16**(11):116024

[57] Thorling CA et al. Multiphoton microscopy and fluorescence lifetime imaging provide a novel method in studying drug distribution and metabolism in the rat liver in vivo. Journal of Biomedical Optics. 2011;**16**(8):086013

[58] Peti-Peterdi J, Burford JL, Hackl MJ. The first decade of using multiphoton microscopy for high-power kidney imaging. American Journal of Physiology. Renal Physiology. 2012;**302**(2):F227-F233

[59] Hall AM et al. Multiphoton imaging of the functioning kidney. Journal of the American Society of Nephrology. 2011;**22**(7):1297-1304

[60] Molitoris BA, Sandoval RM. Multiphoton imaging techniques in acute kidney injury. Contributions to Nephrology. 2010;**165**:46-53

[61] Liang X, Graf BW, Boppart SA. In vivo multiphoton microscopy for investigating biomechanical properties of human skin. Cellular and Molecular Bioengineering. 2011;**4**(2):231-238

[62] Masters B, So P. Confocal microscopy and multi-photon excitation microscopy of human skin in vivo. Optics Express. 2001;**8**(1):2-10

[63] Masters BR, So PT. Multi-photon excitation microscopy and confocal microscopy imaging of In vivo human skin: A comparison. Microscopy and Microanalysis. 1999;**5**(4):282-289

[64] Molitoris BA, Sandoval RM. Techniques to study nephron function: Microscopy and imaging. Pflügers Archiv. 2009;**458**(1):203-209

[65] Dunn KW, Sutton TA, Sandoval RM. Live-animal imaging of renal function by multiphoton microscopy. Current Protocols in Cytometry. 2007. Chapter 12

[66] Tanner GA et al. Micropuncture gene delivery and intravital two-photon visualization of protein expression in rat kidney. American Journal of Physiology. Renal Physiology. 2005;**289**(3):F638-F643

[67] Kolb AL et al. Exogenous gene transmission of Isocitrate dehydrogenase 2 mimics ischemic preconditioning protection. Journal of the American Society of Nephrology. 2018;**29**(4):1154-1164

[68] Li J, Yao Q, Liu D. Hydrodynamic cell delivery for simultaneous establishment of tumor growth in mouse lung, liver and kidney. Cancer Biology & Therapy. 2011;**12**(8):737-741

[69] Corridon PR et al. Bioartificial Kidneys. Current Stem Cell Reports. 2017;**3**(2):68-76

[70] Kim S et al. Current strategies and challenges in engineering a bioartificial kidney. Frontiers in Bioscience (Elite Edition). 2015;7:215-228

[71] Corridon PR. In vitro investigation of the impact of pulsatile blood flow on the vascular architecture of decellularized porcine kidneys. Sci Rep. 2021;**11**:16965. DOI: 10.1038/s41598-021-95924-5

[72] Pantic IV, et al. Analysis of vascular architecture and parenchymal damage generated by reduced blood perfusion in decellularized porcine kidneys using a gray level co-occurrence matrix. Frontiers in Cardiovascular Medicine, 2022;**9**:797283

[73] Gilpin A, Yang Y. Decellularization strategies for regenerative medicine: From processing techniques to applications. BioMed Research International. 2017;**2017**:9831534

[74] Corridon P et al. Time-domain terahertz spectroscopy of artificial skin. SPIE BiOS. SPIE. 2006:**6080**

[75] Corridon PR. Intravital microscopy datasets examining key nephron segments of transplanted decellularized kidneys. Scientific Data. 2022;**9**(1):561. DOI: 10.1038/s41597-022-01685-9